ELSEVIER

Contents lists available at ScienceDirect

Science of the Total Environment

journal homepage: www.elsevier.com/locate/scitotenv





Evaluation of the performance of iron-supplemented pelletised compost as packing material in biofilters for odour abatement in domestic wastewater treatment plants

S. Sáez-Orviz ^{a,b}, R. Lebrero ^{a,b,*}, L. Terrén ^c, S. Doñate ^c, M.D. Esclapez ^c, L. Saúco ^c, R. Muñoz ^{a,b,*}

HIGHLIGHTS

- Composted WWTP sludge proved effective as packing material for odour abatement
- Iron-doped sludge compost showed the best performance among all bed materials tested
- Complete H₂S-NH₃ removal was achieved at EBRTs of 20–60 s regardless of bed material
- At EBRTs of 60–45-30 s, VOC removal exceeded 90 %, independent of the bed material

GRAPHICAL ABSTRACT



ARTICLE INFO

Editor: Paola Verlicchi

Keywords:
Biofilter
Compost
Gas biofiltration
Odour treatment
Wastewater treatment plant

ABSTRACT

Odour emissions from wastewater treatment plants (WWTPs) are a growing concern due to their negative impact on both workers and surrounding communities, with compounds like H_2S , NH_3 and volatile organic contaminants (VOCs) contributing to air pollution and potential health issues. Biological technologies, such as biofilters (BFs), are an environmentally sustainable and cost-effective platform for odour control in WWTPs. The use of byproducts from WWTPs as packed bed material in BFs would support a circular economy within the water sector. This research evaluates the performance of iron-doped pelletised compost from WWTP sludge by-products as packing material in BFs during the removal of H_2S , NH_3 and VOCs at empty bed residence time (EBRT). The experimental set-up consisted of three 8-L BFs filled with commercial iron-doped clay pellets (control), pelletised sewage sludge compost and pelletised sewage sludge compost doped with Fe salts. The three BFs achieved a complete removal of H_2S and NH_3 at EBRTs of 60 and 20 s, while VOC removal exceeded 90 % at EBRTs of 60 and 45 s. The pelletised iron-doped sewage sludge compost supported VOCs removals above 92 % at 60, 45 and 30 s of EBRT. This bed material promoted the growth of genera such as *Thermomonas* and *Thiobacillus* among

^a Institute of Sustainable Processes (ISP), Dr. Mergelina s/n, 470011 Valladolid, Spain

b Department of Chemical Engineering and Environmental Technology, School of Industrial Engineering, University of Valladolid, Dr. Mergelina, s/n, 47011 Valladolid, Spain

^c Depuración de Aguas del Mediterráneo (DAM), Av. Benjamín Franklin, 21, 46980 Paterna, Valencia, Spain

^{*} Corresponding authors at: Institute of Sustainable Processes (ISP), Dr. Mergelina s/n, 470011 Valladolid, Spain; Department of Chemical Engineering and Environmental Technology, School of Industrial Engineering, University of Valladolid, Dr. Mergelina, s/n, 47011 Valladolid, Spain.

E-mail addresses: raquel.lebrero@uva.es (R. Lebrero), raul.munoz.torre@uva.es (R. Muñoz).

others. This research demonstrated the potential of using WWTP sludge by-products as bed materials in BFs for odour abatement, thus supporting the implementation of the circular economy concept within the integrated water cycle.

1. Introduction

Odour emissions from wastewater treatment plants (WWTPs) have become a prominent public concern, as malodours lead to unpleasant discomfort for both plant operators and the surrounding community (Márquez et al., 2021). The most significant odour emissions are produced during the anaerobic biodegradation of organic compounds and the direct discharge of odorous chemicals in wastewater from industrial or domestic sources (Cabeza et al., 2013) (Ren et al., 2019). These malodorous emissions contain nitrogen compounds like ammonia (NH₃), sulphur compounds such as hydrogen sulphide (H₂S) and a variety of volatile organic compounds (VOCs) (Márquez et al., 2021). Some VOCs, combined with NOx, act as precursors to the formation of tropospheric ozone, thus contributing to the urban smog observed above major metropolitan areas (Delhoménie and Heitz, 2005). Additionally, the long-term exposure to these unpleasant odours is likely to be harmful to human health (Lim et al., 2016;, Holmes et al., 2018; Kampa and Castanas, 2008). Typically, H₂S and NH₃ are used as key tracer odorants to monitor odorous emissions from WWTPs. Several cities worldwide have reported significant odour issues from WWTPs, resulting in public complaints and health concerns. For example, in Poland between 2016 and 2021, 41.6 % of Environmental Protection Inspections addressed odour nuisances, with 5.4 % of municipal WWTPs receiving complaints, primarily related to H₂S, ammonia, and VOCs (Czarnota et al., 2023). In Curitiba, Brazil, outdoor H₂S concentrations ranged from 0.14 to 32 μg m-3, exceeding nuisance odour levels and posing potential chronic health risks (Godoi et al., 2018). A WWTP in a coastal tourist area of the Valencian Community (Spain), showed peak H₂S emissions up to 13,939 μg m-³ (10 ppm) at emission points, with higher risk periods between June and August (Luckert et al., 2023). In İzmir (Turkey), despite odour units exceeding 10 OU m-3 at sources, dispersion modelling indicated limited impact on residents, although treatment remains necessary for regulatory compliance and worker safety (Dincer et al., 2020). These examples emphasised the importance of quantifying odour emissions, understanding temporal and spatial variations, and developing effective management to mitigate community impact.

In terms of regulations, there are no specific European regulations setting limit values for H2S, NH3, or VOC emissions from WWTPs. However, some national legislations have set air quality limits based on the total concentration of odorous compounds, expressed in European Odour Units (OUe m⁻³). This metric reflects the combined olfactory impact of all odorous substances present in the air, rather than the sum of individual chemical concentrations, and these limits are typically averaged over a specified exposure period (Bokowa et al., 2021). In certain regions, instead of fixed emission limits, WWTPs must apply best available technologies (BAT) to control odours, often guided by environmental permits and the plant's proximity to residential areas. Emission treatment typically covers both ventilation and point sources such as sludge handling. In contrast, China has set explicit emission limits for H₂S and NH₃ under the national "Emission Standards for Odor Pollutants" (GB 14554-93) (Zhao, 2018), which vary according to facility classification. Meanwhile, in the United States, odour regulations mainly focus on worker safety, with the Occupational Safety and Health Administration (OSHA) imposing occupational exposure limits, including a ceiling of 20 ppm for H₂S and a short-term maximum of 50 ppm for up to 10 min within an 8-h shift (Bokowa et al., 2021) (U.S. Department of Labor, Occupational Safety and Health Administration, n.

When odour pollution preventions is not practical or economically viable, bioprocesses typically emerge as the most cost-efficient solution

for end-of-the-pipe treatment, and have become the most popular technology in the last decade for odour control (Ren et al., 2019), Biotechnologies rely on the natural ability of fungi and bacteria to oxidize odorants at ambient pressure and temperature, without the need of additional chemicals. This makes these processes environmentally sustainable and cost-efficient (Lebrero et al., 2021) (Barbusinski et al., 2017). Biofiltration is one the most commonly employed biotechnologies for odour treatment (Ren et al., 2019), and has been implemented to treat a wide range of gaseous organic and inorganic pollutants in both industrial and municipal emissions (Barbusinski et al., 2017). Biofilters (BFs) rank among the simplest bioreactor configurations for odour treatment, consisting of filter media where odorantdegrading microorganisms attach and form a stable biofilm (Pachaiappan et al., 2022). The concentration of odorous compounds at the BFs inlets varies depending on the treatment process and plant characteristics. Reported concentration ranges are approximately 4 to 75 ppmv for H₂S and 5 to 15 ppmv for NH₃ (Rabbani et al., 2016; Gao et al., 2001). BFs exhibit multiple advantages over their biological and physical-chemical counterparts, such as simplicity, cost-effectiveness, minimal pressure drop and effective removal of pollutants at low concentrations (Barbusinski et al., 2017). In this context, the selection of the BF packed bed is a critical parameter in the design of biofiltration systems, as it represents the primary contributor to the operating costs of odour biofiltration (Lebrero et al., 2013). The most commonly used packing materials in BFs are soil, peat, compost, wood chips or cocopeat. among others. Inert carriers, such as perlite, polyurethane foam, expanded clay or activated carbon, can also be used (Barbusinski et al., 2017). These materials meet most of the process-specific requirements, such as high porosity, large specific surface area (300–1000 m² m⁻³), structural integrity, high moisture retention (40-60 %), low bulk density and mechanical and thermal stability (Pachaiappan et al., 2022). Maintaining an adequate moisture content in the bed material is crucial to support an active microbial community. Thus, insufficient moisture in the BF can lead to biofilm drying, while excessive moisture can cause significant pressure drop and additional gas-liquid mass transfer resistance. Among organic packing materials, compost is the preferred material due to its high microbial diversity, large surface area, excellent air and water permeability, good buffering capacity and low cost (Lebrero et al., 2013). However, a significant drawback of compost-based BFs, is the degradation of the bed material over time, which requires regular replacement every 2 to 3 years (Barbusinski et al., 2017). This not only increases operational costs but also poses challenges in maintaining odour abatement efficiency (Sheoran et al., 2022). A biofilter using pellets as packing material can be easier to manage and operate than a biofilter packed with raw compost. Pellets typically offer uniform shape, improved porosity, and better airflow distribution, which help reducing pressure drop and clogging. Additionally, they often provide a stable surface for biofilm development and facilitate easier maintenance or replacement compared to irregular or loose media (Barbusinski et al., 2017; Ren et al., 2019; Pachaiappan et al., 2022). In this context, the use of pelletised compost sourced from WWTPs as bed material in BFs can reduce costs associated to packing media replacement and promote the circular economy within the WWTP sector by effectively reusing byproducts and minimizing waste. Pelletised compost can increase the lifetime of the packing material by increasing its structural durability. In addition, compost supplementation with Fe salts (typically used in WWTP to precipitate phosphorous) can help capturing H2S more

This research aimed to develop and assess innovative compost-based materials derived from WWTP sludge by-products as sustainable bed

media for biofilters targeting odour abatement. By valorising sludge waste through palletisation (with and without iron salt enrichment) the research promotes a circular economy approach that transforms residual materials into high-performance biofiltration packing material. The effectiveness of these materials was compared to that of commercial iron-doped clay pellets for treating a synthetic gas mixture containing $\rm H_2S,~NH_3,~toluene,~and~\alpha\textsc-pinene,~under~empty~bed~residence~times~(EBRTs)~ranging~from~60~to~20~s.~Additionally,~microbial~community~dynamics~within~each~packing~type~were~investigated~to~evaluate~biological~activity~and~stability.$

2. Materials and methods

This study evaluated the performance of biofiltration systems packed with different materials for the treatment of a synthetic gas stream representative of odorous emissions from a WWTP. The bed materials included a blend of commercial pellets, and two novel compost-based materials derives from sewage sludge: pelletised sewage sludge compost (PSS), pelletised sewage sludge compost with a Fe salts content (PSS-Fe).

2.1. Microorganisms and mineral salt medium

An enriched culture adapted to the biodegradation of H_2S , NH_3 , toluene and α -pinene obtained from a previous experimental system (Sáez-Orviz et al., 2024) was used as inoculum. A sequencing analysis of this microbial consortium was conducted to determine the structure of initial bacterial community.

A mineral salt medium (MSM), simulating the composition of the effluent of a domestic WWTP, was prepared to daily irrigate the BFs, in

order to maintain moisture content and prevent nutrient limitation. The MSM composition was: $66.0~mg~L^{-1}~(NH_4)_2SO_4~(CAS~7783-20-2);~14.4~mg~L^{-1}~K_2HPO_4\cdot 3H_2O~(CAS~16788-57-1);~1.7~g~L^{-1}~NaHCO_3~(CAS~144-55-8)~(all three reagents from Panreac AppliChem, Barcelona, Spain) and <math display="inline">68.5~mg~L^{-1}~glucose~(CAS~50-99-7)~(Sigma-Aldrich, Steinheim, Germany). The pH of the MSM was adjusted to <math display="inline">8.01~\pm~0.28.$

2.2. Gas pollutants

 H_2S , NH_3 , toluene and α-pinene were chosen as representative odorants in WWTP emissions. H_2S (22 % in a N_2 matrix) was acquired from Carburos Metalicos (Spain). NH_3 (30 % in an aqueous matrix) was purchased from Panreac AppliChem (Barcelona, Spain). Toluene and α-pinene, chosen as representative moderately and poorly water-soluble VOCs, were obtained from Sigma-Aldrich.

2.3. Experimental setup and operating procedure

The experimental setup consisted of three independent cylindrical PVC BFswith a packed column volume of 8 L (11.8 cm internal diameter, 78.0 cm height) (Fig. 1). As bed material, both iron-doped raw compost and undoped raw compost were previously pelletised. The raw compost was sourced from a municipal wastewater treatment plant and was initially characterized in terms of particle size distribution and moisture content. The particle size was suitable for pelletisation without further processing. Moisture content was adjusted by spraying water onto the compost until it reached 20–25 %. Pelletisation was performed using a flat die pellet mill equipped with 6 mm diameter matrices and a compression ratio of 1:4. The process was carried out at a working pressure of 20 bar, maintaining the die temperature below 50 °C. After

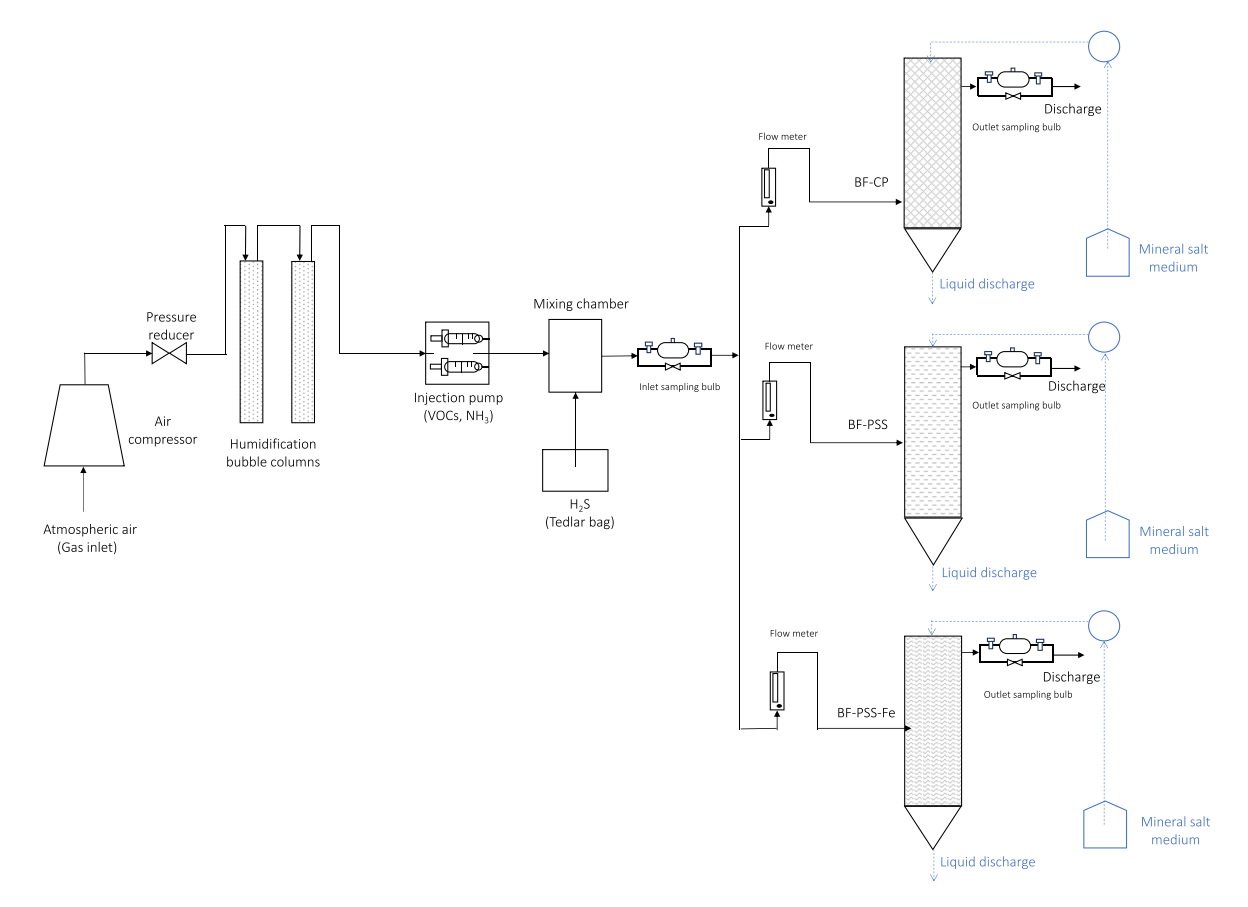


Fig. 1. Outline diagram of the experimental set-up. The solid black lines represent the gaseous streams and the dotted blue lines the aqueous flow. BF-CP refers to the biofilter filled with commercial UgnCleanPellets® as packing material, BF-PSS to the biofilter packed with pelletised sewage sludge compost, and BF-PSS-Fe to the biofilter loaded with pelletised iron-doped sewage sludge compost.

extrusion, the pellets were cut to size by height-adjustable knives mounted on the rollers. To improve mechanical durability and reduce fines, the pellets underwent a cooling phase. This step allowed further moisture reduction and enhanced structural integrity. Final conditioning, including cleaning and cooling, ensured improved mechanical performance and overall pellet quality. Pelletised sewage sludge compost (PSS), pelletised sewage sludge compost with a Fe salts content of 100 g Fe kg⁻¹ dry matter (PSS-Fe), and a mixture of commercial UgnCleanPellets® S.3.5 and UgnCleanPellets® S.1.0 pellets at a 1:4 ratio (CP), were tested (Fig. 2). The iron content of the UgnCleanPellets® mixture was $117.9~{\rm g}~{\rm Fe}~{\rm kg}^{-1}~{\rm dry}$ matter. UgnCleanPellets® are commonly utilized in biofilters and bioscrubbers in Europe due to their consistent performance, high surface area, and durability. The characterization of the PSS and PSS-Fe pellets was performed using internal analytical procedures aligned with UNE-EN ISO standards to evaluate their mechanical durability (%) (UNE-CEN/TS 15210-1-EX), bulk density (kg m⁻³) (UNE-CEN/TS 15103 EX), moisture content (%) (UNE-CEN/TS 14774-2 EX), and dimensions (length and diameter, both expressed in mm) (UNE-EN ISO 17829) (Table 1).

The airflow was generated using an air compressor (Puska-HP3, Vizcaya, Spain) and was controlled by calibrated air rotameters (Aalborg, NY, USA) before entering the BFs. To prevent the inlet air from drying out the compost, the gaseous stream was pre-humidified with two 1 m bubble columns in series.

The synthetic malodorous emissions to be treated was formulated to have similar odorant levels to those measured in a full-scale Spanish WWTP in the mediterranean area designed to treat 21.000 $\mathrm{m}^3~\mathrm{d}^{-1}$ (WWTP-Sagunto, Valencia, Spain): 25.0 ppm_v of H₂S, 27.0 ppm_v of NH₃, 2.5 mg m⁻³ of toluene and 2.5 mg m⁻³ of α -pinene. The gas mixture of H₂S:N₂ was introduced into the inlet air stream by means of a 25 L Tedlar bag (Sigma-Aldrich) using a peristaltic pump (Watson-Marlow Limited, Falmouth, UK). Liquid NH₃ and VOCs were introduced into the inlet air stream using a syringe pump (Fusion 100, Chemyx Inc., TX, USA) equipped with a 25 mL and 5 mL glass syringes (Hamilton, CA, USA). Before inoculation, an abiotic test was conducted for one week by monitoring the inlet and outlet gas concentrations of H2S, NH3 and VOCs to ensure the absence of removal mechanisms such as adsorption or photolysis, and to check the microbiological activity of the compost. Each BF was inoculated with 500 mL of acclimated biomass via irrigation from the top of the BF at 24 $\rm mL~min^{-1}$, and initially operated at an EBRT of 60 s. The experimental system was maintained at constant room temperature (25 °C). The impact on the odorant removal efficiency (RE) was assessed at 60, 45, 30 and 20 s EBRT for 93 days (Table 2).

The gas concentration of H_2S , NH_3 and VOCs was measured three times a week in the inlet and outlet of the BFs. Liquid samples (~ 30 mL) were also taken from the leachate of the BFs three times a week to monitor the pH, concentration of Fe, SO_4^{2-} , NO_2^{-} , NO_3^{-} , the dissolved total organic and inorganic carbon (TOC and IC, respectively) and dissolved total nitrogen (TN). Besides, the pressure drop across the packed

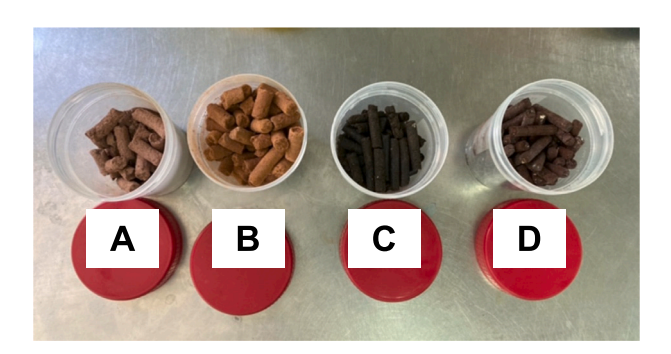


Fig. 2. Packing materials tested in this work. (A) UgnCleanPellets® S.1.0, (B) UgnCleanPellets® S.3.5, (C) pelletised sewage sludge compost (PSS) and (D) pelletised sewage sludge compost doped with Fe salts (PSS-Fe).

bed was measured three times a week in each BF.

2.4. Analytical methods

H₂S and NH₃ were measured in the air stream using a Dräger X-am 5000 electrochemical sensor (Drägerwerk, Lübeck, Germany). For H₂S, the measurement range was 0 to 200 ppm, with a sensitivity threshold of 1 ppm; while for NH₃, the measurement range was 0 to 300 ppm, also with a sensitivity threshold of 1 ppm. Due to an interference caused by H₂S in the electrochemical determination of NH₃ concentration, the H₂S inlet was stopped for 15 min for NH₃ analysis. For VOCs determination, sampling was performed by solid phase microextraction (SPME) in the inlet and outlet of each BF. Gas samples were collected in 250 mL glass bulbs (Sigma-Aldrich) and preconcentrated for 15 min using 85 μm PDMS/Carboxen SPME fibers (Supelco, Bellefonte, PA, USA). The SPME fibers were injected in a GC-FID (HP 6890 Series, Hewlett Packard, CA, USA) equipped with a SupelcoWax (15 m \times 0.25 mm \times 0.25 μ m) capillary column. Oven, injector and detector temperatures were maintained at 60, 280 and 250 $^{\circ}$ C, respectively. The flowrates of H₂ and air were fixed at 30- and 300-mL min⁻¹, respectively. Helium was employed as the carrier gas at 2 mL min⁻¹.

The pH of the BF leachates was determined using a pH-meter (Crisson, Barcelona, Spain). SO_4^{2-} , NO_2^{-} and NO_3^{-} concentration was evaluated by HPLC-IC employing a Waters 515 HPLC pump coupled with a conductivity detector (Waters 432) and fitted with an IC-Pak Anion HC column (4.6 × 150 mm) and an IC-Pak Anion Guard-Pak (Waters). Before analysis, samples were diluted and filtered with a nonsterile nylon 0.22 µm syringe filter (Sigma-Aldrich). Samples were eluted isocratically at 2 mL min⁻¹ with a solution of water/acetonitrile/ n-butanol/buffer at 84/12/2/2 % ν/ν at a temperature of 25 °C. TOC, IC and TN were determined using a TOC-VCSH analyser (Shimadzu, Tokyo, Japan) coupled with a total nitrogen chemiluminescence detection module (TNM-1, Shimadzu, Tokyo, Japan). Prior to analysis, samples were diluted and filtered with a nonsterile nylon 0.45 µm syringe filter (Sigma-Aldrich). The pressure drop was assessed using a U-shaped gauge with water as a manometric fluid and was quantified in mm of H2O with a sensitive of 1 mm-H₂O. Results were expressed as mm-H₂O per m⁻¹ of bed height.

The concentration of Fe in the leachate from the BFs was determined by atomic spectroscopy by means of inductively coupled plasma-optical emission spectroscopy (ICP-OES, HC 7500 cc, Agilent, USA) according to the internal procedures of the Instrumental Techniques Laboratory (LTI-UVa). Samples from the MSM, and leachate of PSS-BF and PSS-Fe-BF under steady state operation at 60, 45 and 30 s of EBRT were collected to check whether the iron salts were retained in the compost pellet or dissolved in the liquid phase. Those EBRTs were selected based on the optimal BF performance in terms of odorant abatement. Prior to analysis, samples were filtered with a nonsterile nylon 0.45 μm syringe filter (Sigma-Aldrich).

2.5. Microbial community sequencing analysis

Different microbial samples were taken for metagenomic amplicon sequencing analysis. Samples of the inoculum and the initial bed materials (CP, PSS and PSS-Fe) were collected before inoculation. Additionally, samples were obtained on the final experimental day of each BF (BF-CP, BF-PSS and BF-PSS-Fe). The biomass was centrifuged at 13,000 $\times g$ for 15 min and the resultant pellet was employed for DNA extraction. DNA was isolated using the FastDNATM SPIN Kit for Soil (MP Biomedicals, WA, USA). The concentration of the DNA recovered after extraction ranged from 12 to 28.4 ng/ μ L. Novogene (Cambridge, UK) conducted the library preparation and Illumina Mini Seq amplicon metagenomics. For quantification, Qubit and real-time PCR were used, while size distribution was detected with a bioanalyzer. Paired-end reads were combined using FLASH V1.2.11 (Magoč and Salzberg, 2011). Sequence analysis was conducted using Uparse software

 Table 1

 Parameters analysed in the characterization of the pellets.

Compost packing material	Length (mm)	Diameter (mm)	Mechanical durability (%)	Bulk density (kg m ⁻³)	Moisture content (%)
PSS	22.7	5.8	91.7	680	16.1
PSS-Fe	14.9	5.6	96.1	790	14.9
UgnCleanPellets® S.3.5	10-30	7	Not data available	450	< 10 %
UgnCleanPellets® S.1.0	10–30	7	Not data available	450	< 10 %

Table 2Summary of the operational parameters during the evaluation of the EBRT influence.

EBRT (s)	Elapsed time (days)	$Q_{gas/BF}$ (L min $^{-1}$)	$Q_{gas/}$ $_{total}$ (L min $^{-1}$)	H ₂ S:N ₂ (mL min ⁻¹)	H ₂ S (mg min ⁻¹)	H ₂ S loading rate (g m ⁻³ h ⁻¹)	$ m NH_3$ (mg $ m min^{-1}$)	NH ₃ loading rate (g m ⁻³ h ⁻¹)	Toluene (mg min ⁻¹)	Toluene loading rate (g m ⁻³ h ⁻¹)	α -pinene (mg min ⁻¹)	α -pinene loading rate (g m ⁻³ h ⁻¹)
60	38	8.0	24.0	2.7	3.7	26.2	2.2	15.3	0.06	0.42	0.06	0.42
45	29	10.7	32.0	3.6	4.9	34.9	2.9	20.3	0.08	0.56	0.08	0.56
30	20	16.0	48.0	5.5	7.4	53.4	4.3	30.5	0.12	0.85	0.12	0.85
20	6	24.0	72.0	8.2	11.1	78.6	6.5	45.7	0.18	1.27	0.18	1.27

V.7.0.1001 (Edgar, 2013). Sequences with 97 % similarity were grouped into the same Operational Taxonomic Units (OTUs) according to the SILVA gene reference database (Quast et al., 2013).

2.6. Data treatment and statistical analysis

Removal efficiencies (RE) for H₂S, NH₃ and VOCs were determined using the following equation (Eq. 1):

$$\text{\%RE} = 100 \times \left(\frac{C_{in} - C_{out}}{C_{in}}\right)$$

where C_{in} and C_{out} represent the inlet and outlet concentrations, respectively, measured in ppm_v for H₂S and NH₃, and in mg m⁻³ for VOCs.

Elimination capacities (EC) were calculated for the odorous compounds based on the following equation (Eq. 2):

$$EC = \frac{(C_{in} - C_{out}) \times Q_g}{H \times S}$$

where C_{in} and C_{out} are the inlet and outlet concentrations expressed in g m⁻³; Q_g is the air flow rate (m³ h⁻¹); H is the height of the reactor expressed in m and S is the cross-section area of the reactor (m²). EC results are expressed in g m⁻³ h⁻¹.

An analysis of variance (ANOVA) was conducted. Fischer's Least Significant Difference (LSD) was used to determine significant differences between the data. A level of p < 0.05 was considered significant. Analysis was performed using StatPlus v7.8.11 statistical software.

Thus, RE and EC are related but represent different performance aspects. RE expresses the percentage of contaminant removed, while EC quantifies the absolute amount removed per unit volume and time. Although a higher RE often leads to a higher EC, the relationship is not strictly linear, as EC also depends on airflow rate and reactor dimensions. Both metrics are complementary and necessary for a comprehensive evaluation of system performance.

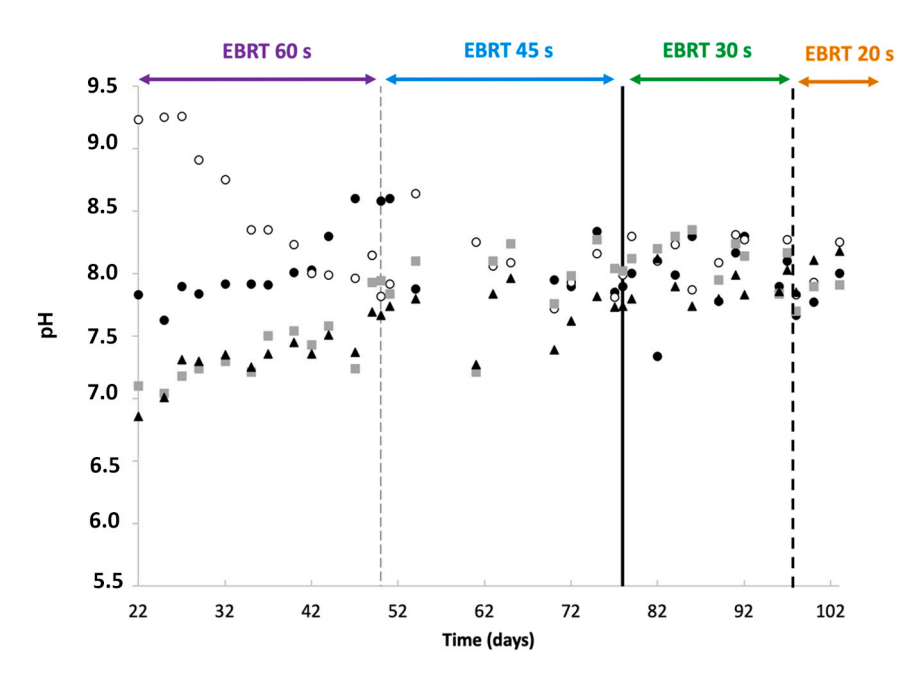


Fig. 3. Time course of the pH in the MSM (●) and in the leachate of (○) BF-CP, (■) BF-PSS and (▲) BF-PSS-Fe under decreasing EBRTs. Horizontal arrow lines at the upper part of the figure represent the empty bed residence time of the gas during this operational stage. Statistically significant differences were observed at EBRT 60 s between BF-CP/MSM and the sewage sludge-based biofilters (BF-PSS and BF-PSS-Fe); at shorter EBRTs, no significant differences were found (p < 0.05).

3. Results and discussion

3.1. Influence of the EBRT on the pH of the leachate

The liquid volume daily irrigated was completely retained within the packing material until day 22, when leachate from the BFs occurred for the first time (Fig. 3).

The pH of the MSM used for irrigation was 8.01 \pm 0.28, while the average pH values of the leachate under steady-state operation at 60 s EBRT were 8.23 \pm 0.40, 7.78 \pm 0.40 and 7.65 \pm 0.31 in BF-CP, BF-PSS and BF-PSS-Fe, respectively. BF-CP initially exhibited the highest leachate pH, with a mean value of 9.08 \pm 0.21 during the first 10 days. Over time, the pH gradually decreased, eventually aligning with that of the MSM. During the first week, fungal growth was visually detected on the packing material of BF-CP but disappeared as the pH decreased. These fungi were likely inherent to the commercial pellets, as no fungal growth was observed in BF-PSS or BF-PSS-Fe. Thus, their growth was likely fostered by the high humidity and elevated pH values. Under steady state operation at EBRTs of 45, 30 and 20 s, the pH remained at average values of 8.07 \pm 0.22, 8.01 \pm 0.24 and 7.82 \pm 0.21 in BF-CP, BF-PSS and BF-PSS-Fe, respectively. The pH levels observed were favorable to the proliferation of bacteria involved in the degradation of VOCs, as well as autotrophic bacteria responsible for the oxidation of NH₃ and H₂S (Chaudhary et al., 2023).

3.2. Iron concentration in the leachate from the BFs

Several studies have incorporated iron into compost in various forms, such as Fe particles, Fe_2O_3 , $\text{Fe}(\text{NO})_3$, FeSO_4 or FeCl_3 , to mitigate odorous emissions during compost production (Pan et al., 2024). For instance, Chen et al. (2024) added 0.05 % (w/w) zero-valent iron, 3 % (w/w) H_2O_2 and 0.5 % (w/w) ascorbic acid into compost, resulting in a 51 % reduction in ammonia emissions and a 43 % reduction in VOC emissions.

To assess the loss of Fe from the pellets, the Fe concentration was analysed in the inlet MSM ($< 0.025 \text{ mg L}^{-1}$) and in the BFs leachate (Table 3). Fe concentrations in the BF-PSS leachate averaged 15.4, 4.67 and 8.12 mg L⁻¹ at EBRTs of 60, 45 and 30 s, which was attributed to the inherent presence of Fe in the pelletised sewage sludge compost. In the BF-PSS-Fe leachate, Fe concentrations were 31.8, 23.8 and 7.51 mg L^{-1} at 60, 45 and 30 s of EBRs, respectively. The initial concentration of Fe in the pelletised sewage sludge compost with iron salts ranged from 60 to 100 g Fe kg⁻¹ dry matter. Thus, although some loss of these salts was observed in the leachate, it remained low compared to the initial PSS-Fe content. Consequently, the lower iron concentration observed at shorter EBRTs, particularly at 30 s, may be attributed to the retention of iron within the pellet matrix This retention is advantageous for the BF performance, as it suggests that the supplemented iron remains available within the system, potentially supporting microbial activity and enhancing the degradation of pollutants over time.

3.3. Influence of the EBRT on inorganic and organic carbon concentration in the leachate

The TOC concentration in the leachate was initially high during the start-up of the BFs and gradually decreased over time in the three BFs

Table 3 Fe concentration (mg $\rm L^{-1}$) in the MSM, and in the leachate of BF-PSS and BF-PSS-Fe.

EBRT (s)	Fe concentration (mg L ⁻¹)				
	MSM (irrigation)	BF-PSS	BF-PSS-Fe		
60	< 0.025	15.4	31.8		
45	_	4.7	23.8		
30	-	8.1	7.5		

(Fig. 4-A). Significant differences were observed in the average TOC concentrations at the end of the operating period at an EBRT of 60 s, with values of 3960 \pm 829, 7730 \pm 2098 and 9496 \pm 1113 mg L $^{-1}$ in BF-CP, BF-PSS and BF-PSS-Fe, respectively. Since compost is primarily composed of organic matter, these high TOC values could be attributed to carbon leaching. This leaching progressively decreased over time in the three BFs, reaching the lowest TOC concentrations at an EBRT of 20 s: 405.8 \pm 47.1, 659.9 \pm 38.7 and 1117.7 \pm 204.3 mg L $^{-1}$ in BF-CP, BF-PSS and BF-PSS-Fe, respectively.

The average inlet concentration of IC in the MSM was 214.9 \pm 26.4 mg L⁻¹ (Fig. 4-B). At 60 s EBRT, the IC concentrations in the leachates were higher in the BF-PSS and BF-PSS-Fe (630.4 \pm 211.2 and 489.7 \pm 131.4 mg L⁻¹, respectively) than in the BF-CP (306.1 \pm 150.5 mg L⁻¹), likely due to the initial composition of the pellets. These higher initial concentrations could be related to the absorption and accumulation of IC within the system during the first 22 days, before leachate production began. Since no leachate was produced during this initial period, the IC concentration in the system gradually built up since MSM contained 1.7 g L⁻¹ NaHCO₃. Once leachate started to be produced after day 22, the accumulated IC was released, leading to a decrease in IC concentration over time. At EBRTs of 45, 30, and 20 s, the IC concentrations in the leachates levelled off, showing similar mean values of 206.0 \pm 85.4 in BF-CP, 293.5 \pm 83.2 in BF-PSS, and 290.8 \pm 93.7 mg L⁻¹ in BF-PSS-Fe. This stabilization of IC levels suggests that the system reached an equilibrium, where microbial processes, along with the characteristics of the pellet material, regulated the retention and release of IC.

3.4. Influence of the EBRT on H₂S and NH₃ removal

The mean H_2S concentration in the inlet gaseous stream was $31.4\pm4.9~ppm_v$ (Fig. 5-A). During the 7 days of abiotic experiment (Ab), no H_2S adsorption or photolysis occurred. The addition of the compost and UgnCleanPellets® pellets as packing bed material (Rf) in the biofilters resulted in a $100~\%~H_2S$ -RE in BF-CP and BF-PSS-Fe, while H_2S removal remained at $41.2\pm3.5~\%$ in the BF-PSS. The absence of iron in BF-PSS likely contributed to this lower removal efficiency, as iron is a critical cofactor for sulphur-oxidizing bacteria involved in H_2S degradation and H_2S chemical precipitation. In contrast, the presence of iron in BF-PSS-Fe and in the commercial pellets supports microbial processes, enabling complete H_2S degradation even without inoculation, and chemical H_2S precipitation.

After inoculation, BF-CP and BF-PSS-Fe exhibited complete H2S removal across all tested EBRTs. BF-PSS supported a H₂S-RE of 94.9 \pm 2.5 % during the first 9 days following inoculation, after which it remained at 100 % for all EBRTs evaluated. These results demonstrate the outstanding efficiency of the biofilters engineered in this work for the aerobic degradation of H2S at low concentrations and at EBRTs as low as 20s. This was likely attributed to the high aqueous solubility of H₂S, which facilitated a large gas-liquid concentration gradient (Vikrant et al., 2018) (Lebrero et al., 2014). Similarly, Zhu et al. (2017) achieved H₂S-RE of 100 % in a 20 L BF packed with a mixture of mature compost, porous perlite and inorganic binder at inlet loading rates of 49.5-80 g $m^{-3} h^{-1}$ at EBRTs of 29–121 s. Likewise, Rabbani et al. (2016) operated a 28 L BF packed with acid resistant polyethylene at a working EBRT of 60 s treating 31.85 ppm_v of H₂S with H₂S-REs as high as 94.4 %. Our study therefore confirmed the high efficiency of BFs in abating low H₂S concentrations at EBRTs ranging from 60 to 20 s.

As consistently reported in previous studies, gaseous $\rm H_2S$ is absorbed in the biofilm and compost and subsequently dissociated to $\rm HS^-$ at neutral/slightly alkaline pH. The $\rm HS^-$ diffuses into the interior of the biofilm attached to the compost, thereby becoming available to sulphuroxidizing bacteria (SOB), and is then oxidized to sulphates primarily due to the metabolism of aerobic bacteria (Barbusinski et al., 2017; Bharathi, 2018). In our system, $\rm SO_4^{2-}$ concentrations were measured in the leachate of the three BFs (Fig. 5-B). In BF-CP, mean sulphate levels were $\rm 8362 \pm 5681, 15,692 \pm 1391, 14,546 \pm 1368$ and $\rm 12,608 \pm 731$ mg $\rm L^{-1}$

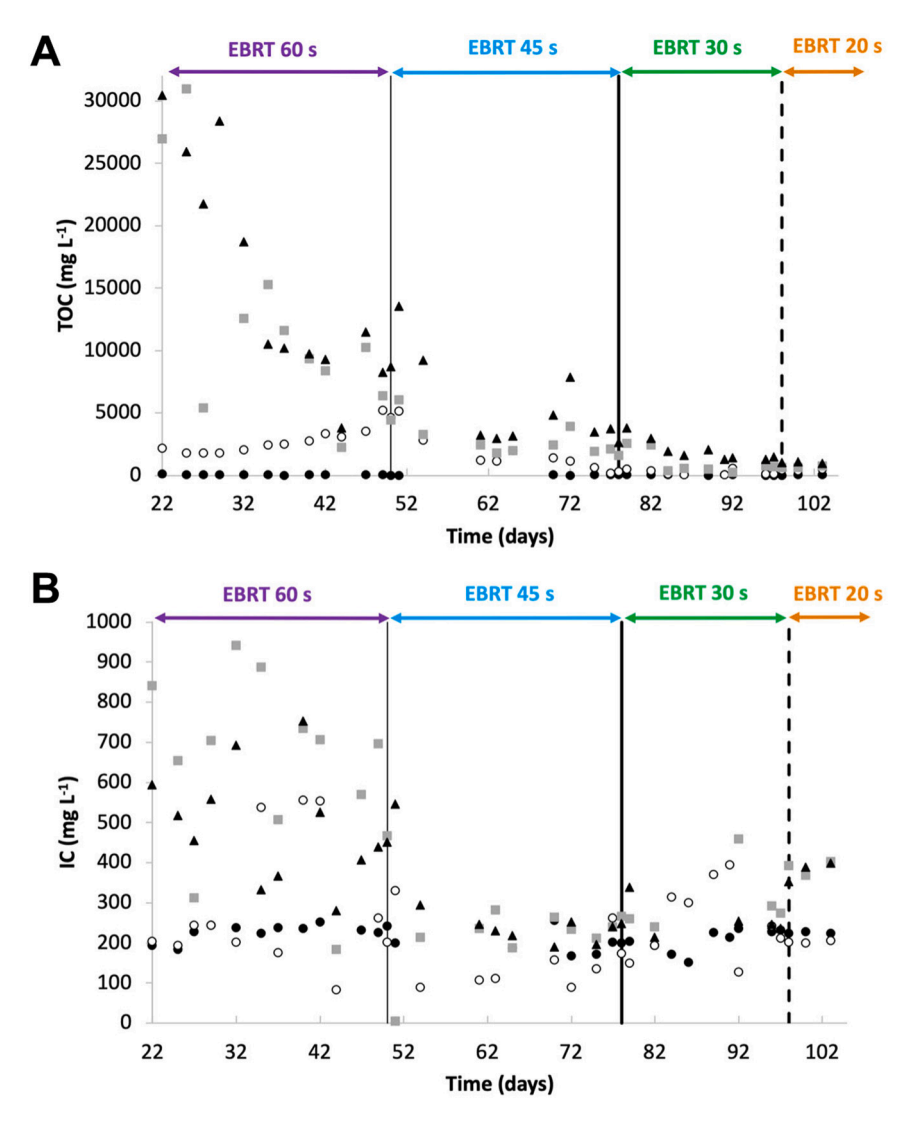


Fig. 4. Time course of the concentrations of inorganic carbon (IC) (A) and total organic carbon (TOC) (B) in the fresh MSM (●) and in the leachate of (○) BF-CP, (■) BF-PSS and (▲) BF-PSS-Fe under decreasing EBRTs. Horizontal arrow lines at the upper part of the figure represent the empty bed residence time of the gas during this operational stage.

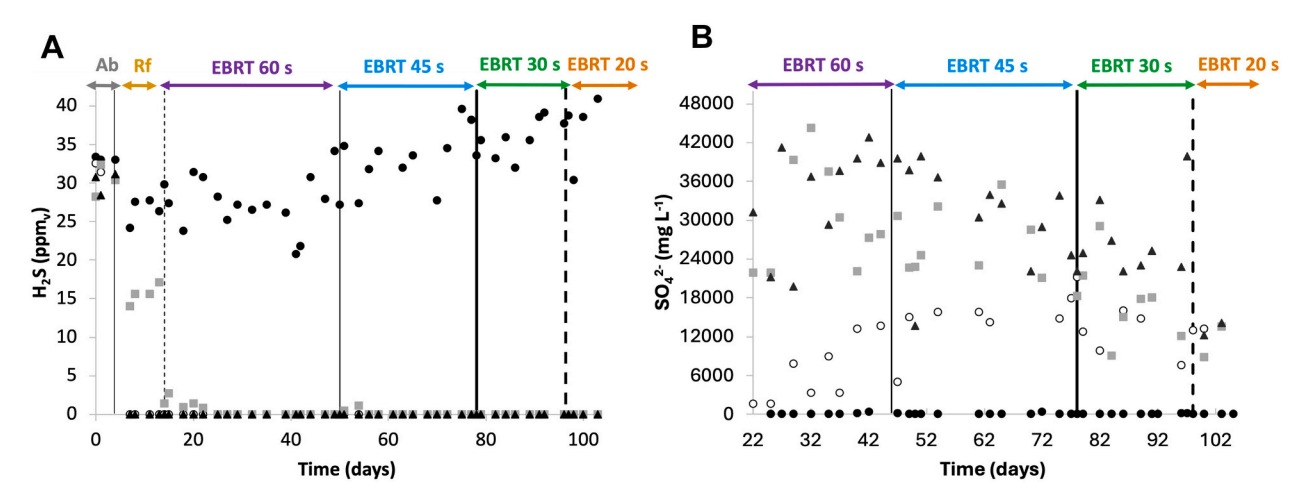


Fig. 5. Time course of the concentrations of (A) H_2S and (B) sulphate in the inlet gas stream and irrigation MSM (\bullet), and in the outlet gas stream or leachate of BF-CP (\circ), BF-PSS (\blacksquare) and BF-PSS-Fe (\blacktriangle) at decreasing EBRTs. (Ab) refers to the abiotic period and (Rf) to the addition of the packing material to the BFs prior to inoculation. Horizontal arrow lines at the upper part of the figure represent the empty bed residence time of the gas during this operational stage.

at EBRTs of 60, 45, 30 and 20 s, respectively. Sulphate concentrations in BF-PSS and BF-PSS-Fe were significantly higher than in BF-CP and decreased as the EBRT was reduced. At 60 s EBRT, SO_4^{2-} values reached 26,904 \pm 3585 mg L^{-1} in BF-PSS and 37,738 \pm 3615 mg L^{-1} in BF-PSS-Fe. Sulphate concentrations progressively decreased at EBRT of 45 s (24,236 \pm 2720 and 33,232 \pm 3449 mg L^{-1}), 30 s (18,817 \pm 4980 and 24,131 \pm 1626 mg L^{-1}) and 20 s (17,401 \pm 6164 and 13,178 \pm 973 mg L^{-1}) for BF-PSS and BF-PSS-Fe, respectively.

The average inlet concentration of NH3 over the experimental period was 32.1 \pm 0.6 ppm_v. During the abiotic tests, due to a malfunction of the NH₃ sensor, data collection was not possible. However, preliminary abiotic tests conducted in a similar experimental set-up showed negligible NH₃ adsorption and photolysis (Sáez-Orviz et al., 2024). Through the experimental period, all three BFs achieved complete NH₃ removal (Fig. 6-A). However, significant differences were found in the leachate TN concentrations between BF-CP and BF-PSS/PSS-Fe at an EBRT of 60 s (Fig. 6-B). From day 22nd onward (when leachate appeared), TN values increased from 830 \pm 302 to 2476 \pm 859 mg L $^{-1}$ in BF-CP and decreased from $10{,}018 \pm 2630$ to 4561 ± 1898 mg L $^{-1}$ in BF-PSS, and from $10{,}562$ \pm 2107 to 4432 \pm 459 mg L⁻¹ in BF-PSS-Fe. The high TN values in compost-based BFs may be attributed to organic nitrogen leaching, while the increase in TN concentrations in BF-CP can be explained by a combined accumulation of ammoniacal nitrogen and a slow-release of nitrogen from UgnCleanPellets®. Hence, the differing TN concentration patterns between CP and PSS/PSS-Fe may be attributed to the different composition of the pellets. TN concentration continued to decrease as the EBRT decreased, achieving the lowest values at an EBRT of 20 s (767 \pm 27, 1092 \pm 124 and 1487 \pm 394 mg L⁻¹ for BF-CP, BF-PSS and BF-PSS-Fe, respectively), likely due to the gradual depletion of nitrogen in the pellets.

Nitrite and nitrate concentration was monitored in the leachate of the BFs to assess the nitrifying activity of the microorganisms adhered to the packing material (Fig. 6-C-D). The nitrification process involves two distinct steps, each driven by specific bacterial groups. In the first step, ammonium is oxidized to nitrite by bacteria primarily from the genera Nitrosomonas and Nitrosococcus. In the second step, nitrite is further converted into nitrate by microorganisms, predominantly from the genus Nitrobacter (Gupta et al., 2021). Average NO₂ concentrations of $176.6 \pm 21.4, 149.8 \pm 11.8$ and 162.6 ± 14.9 4 mg L $^{-1}$ were recorded in the leachate of BF-CP, BF-PSS and BF-PSS-Fe, respectively, during the complete operating period (Fig. 6-C). Similarly, NO₃ concentration remained constant in the leachate of all three BFs independently of the EBRT tested, with mean values of 222.4 \pm 9.1, 220.8 \pm 38.6 and 235.2 \pm 15.2 mg L $^{-1}$ in BF-CP, BF-PSS and BF-PSS-Fe, respectively. The microbial community analysis revealed the presence of ammonia-oxidizing bacteria (AOB) and nitrite-oxidizing bacteria (NOB) in the biofilms at the end of the experiment, such as Nitrospira (relative abundance of 0.51 %, 0.22 % and 0.40 % in BF-CP, BF-PSS and BF-PSS-Fe, respectively) and Nitrosomonas (relative abundance of 0.20 %, 0.73 % and 0.11 % in BF-CP, BF-PSS and BF-PSS-Fe, respectively).

Overall, $\rm H_2S$ and $\rm NH_3$ ECs were identical in the three BFs as a result of the complete oxidation of both odorants (Table 4). At the lowest EBRT of 20 s, the maximum $\rm H_2S$ -EC of 9.6 g m⁻³ h⁻¹ and $\rm NH_3$ -EC of 3.9 g m⁻³ h⁻¹ were achieved. Several authors have analysed the simultaneous removal of $\rm H_2S$ and $\rm NH_3$ in BFs. For instance, Park et al. (2008) operated a 1.0 L BF packed with a commercial inorganic/polymeric composite carrier. These authors evaluated inlet loading rates ranging from 1.9 to 6.4 g m⁻³ h⁻¹ for $\rm H_2S$ and from 1.1 to 3.0 g m⁻³ h⁻¹ for $\rm NH_3$, operating at EBRTs ranging from 120 to 60 s. The maximum ECs achieved accounted for 2.7 g m⁻³ h⁻¹ for $\rm NH_3$ and 6.4 g m⁻³ h⁻¹ for $\rm H_2S$, in the

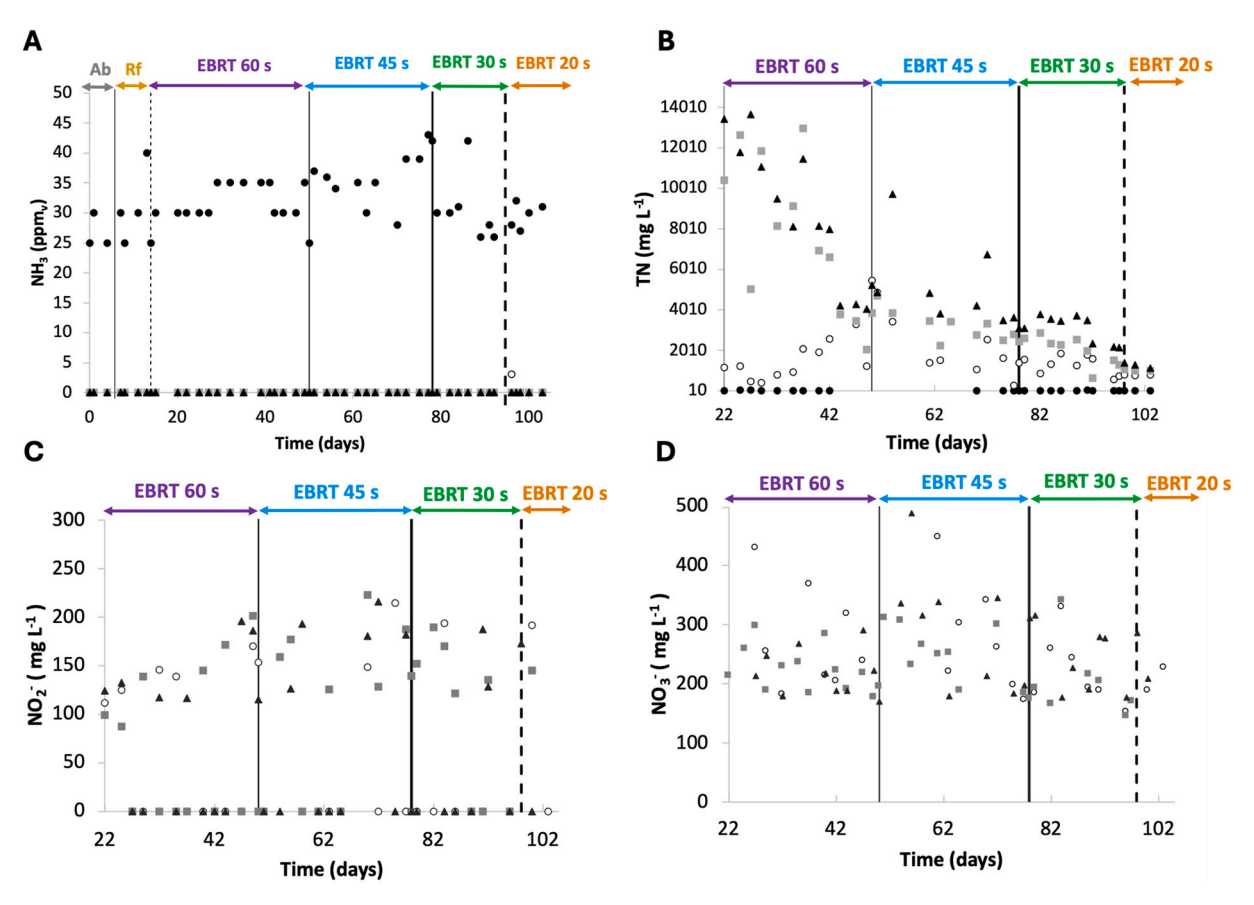


Fig. 6. Time course of the (A) gaseous NH $_3$ concentration and (B) TN concentrations, (C) nitrite concentrations and (D) nitrate concentrations in the inlet gas (\bullet) and in the outlet gas and leachates of BF-CP (\circ), BF-PSS (\blacksquare) and BF-PSS-Fe (\blacktriangle) at decreasing EBRTs. (Rf) to the initial period of operation with the packing material in the BFs prior to inoculation. Horizontal arrow lines at the upper part of the figure represent the empty bed residence time of the gas during this operational stage.

Table 4 H_2S and NH_3 steady state elimination capacities (EC; g m⁻³ h⁻¹).

${ m H_2S~EC~(g~m^{-3}~h^{-1})}$					
EBRT (s)	BF-CP	BF-PSS	BF-PSS-Fe		
60	2.4	2.4	2.4		
45	3.8	3.8	3.8		
30	6.2	6.2	6.2		
20	9.6	9.6	9.6		

$NH_3 EC (g m^{-3} h^{-1})$					
EBRT (s)	BF-CP	BF-PSS	BF-PSS-Fe		
60	1.3	1.3	1.3		
45	2.0	2.0	2.0		
30	2.7	2.7	2.7		
20	3.9	3.9	3.9		

same order of magnitude to those observed in our study. Vela-Aparicio et al. (2021) operated a 6.6 L BF packed with compost mixtures made from chicken manure and lignocellulosic residues (pruning waste, sugarcane bagasse and rice husk) treating a gaseous stream with $\rm H_2S$ and NH $_3$ concentrations of 52–260 mg m $^{-3}$ and 2–10 mg m $^{-3}$, respectively. These authors obtained the highest EC for both compounds at an EBRT of 25 s (32.0 for $\rm H_2S$ and 1.2 g m $^{-3}$ h $^{-1}$ for NH $_3$), corresponding to REs of 87 % for H $_2S$ and 86 % for NH $_3$.

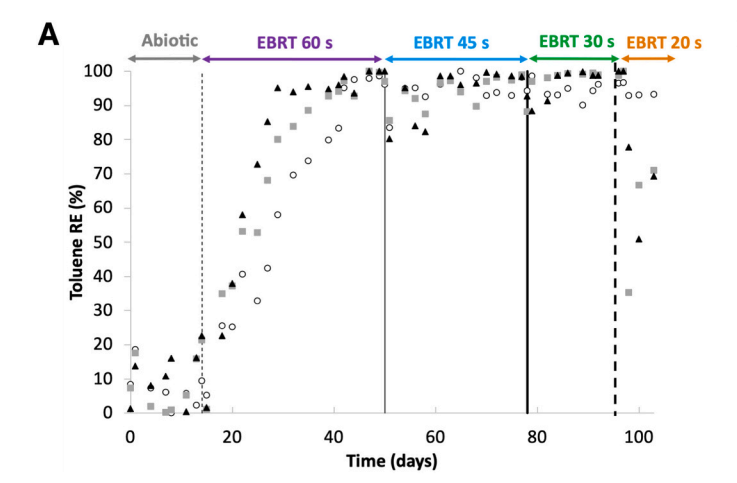
3.5. Influence of the EBRT on VOCs removal

The average inlet concentration of toluene during the experimental period was 3.69 ± 0.58 mg m⁻³. At an EBRT of 60 s, steady state was achieved by day 29 in the three BFs, with average toluene REs of 97.3 \pm 0.4 % in BF-CP, 98.5 \pm 1.3 % in BF-PSS, and 99.0 \pm 0.7 % in BF-PSS-Fe (Fig. 7-A). At an EBRT of 45 s, steady state was reached after 13, 11 and 5 days in BF-CP, BF-PSS and BF-PSS-Fe, respectively, with corresponding toluene-REs of 94.5 \pm 2.0 %, 97.9 \pm 0.8 % and 98.2 \pm 1.2 %. These efficiencies were maintained during operation at an EBRT of 30 s, reaching values of 94.0 \pm 2.0 % in BF-CP. 98.9 \pm 0.4 % in BF-PSS and 99.3 ± 0.6 % in BF-PSS-Fe, highlighting the superior performance of the Fe-doped pelletised compost. However, at an EBRT of 20 s, toluene RE in BF-CP remained similar to the previous stage, while BF-PSS and BF-PSS-Fe experienced a gradual decline. This decrease was associated to operational problems, including partial flooding in BF-PSS caused by compost pellet disintegration and compaction. Consequently, the final toluene REs achieved at 20 s EBRT dropped to 70.9 % in BF-PSS and 69.3 % in BF-PSS-Fe. These findings highlight the need for further

research to improve the structural stability of pelletised compost.

Inlet concentration of α -pinene in the synthetic odorous stream averaged 3.00 \pm 0.63 mg m⁻³. Steady state REs of α -pinene were achieved by day 31, 26 and 19 in BF-CP, BF-PSS and BF-PSS-Fe, respectively, which confirmed the superior performance of the Fe-doped pelletised compost. α-pinene typically requires longer periods to degrade than toluene, as it is a recalcitrant monoterpene (Kleinheinz and Bagley, 1999), with high hydrophobicity and a complex cyclic structure that limits its bioavailability to bacteria (Cantera et al., 2022). However, employing a pre-acclimated inoculum for VOC biodegradation significantly reduced the star-up time, achieving toluene degradation within 5 days and α-pinene degradation within 12 days. At an EBRT of 60 s, $\alpha\text{-pinene}$ REs were 96.5 \pm 4.9 % in BF-CP, 98.5 \pm 1.3 in BF-PSS and 100 % in BF-PSS-Fe. The reduction in EBRT to 45 s did not significantly affect α -pinene REs, that remained at comparable levels of 98.8 \pm 1.8 %, 100 % and 100 % in BF-CP, BF-PSS and BF-PSS-Fe, respectively. However, at 30 s EBRT, steady α-pinene-REs declined significantly in BF-CP to 31.7 \pm 1.5 %, while BF-PSS and BF-PSS-Fe maintained high REs of 99.4 \pm 1.1 % and 92.5 \pm 0.8 %, respectively. Finally, a gradual decline in RE from 34.1 % to 13.0 % in BF-CP, from 4.7 to 1.8 % in BF-PSS and from 62.7 to 31.3 % in BF-PSS-Fe was recorded under process operation at 20 s EBRT. This reduction was likely due to insufficient contact time between the gas phase and the biofilm containing VOC-degrading bacteria, leading to a decrease in the removal of α -pinene. Similar findings were reported by other authors during the biodegradation of gaseous toluene in fungal and bacterial BF (Rajamanickam and Baskaran, 2017; Cheng et al., 2016)

The VOCs-ECs depended on the bed material used in the BFs (Table 5). Toluene inlet loading rates were 0.22, 0.27, 0.40 and 0.57 g $\mbox{m}^{-3}\ \mbox{h}^{-1}$ at EBRTs of 60, 45, 30 and 20 s, respectively. The highest toluene ECs were achieved in all BFs at an EBRT of 20 s, reaching 0.53 \pm 0.00, 0.40 \pm 0.00 and 0.41 \pm 0.03 57 g $m^{-3}\,h^{-1}$ in BF-CP, BF-PSS and BF-PSS-Fe, respectively. Compared to previous studies, the toluene loading rates in this work were significantly lower as a result of the low VOC concentrations tested. For instance, Rene et al. (2018) operated a 1.4 L BF with sieved compost (3–6 mm) and ceramic beads (4–6 mm) mixed in a 6:4 vol. ratio as packing material, achieving maximum toluene EC of 29.2 g m⁻³ h⁻¹ at an inlet loading rate of 53.8 g m⁻³ h⁻¹. Similarly, Rajamanickam and Baskaran (2017) operated a 1.1 L BF packed with ceramic beads and cow dung compost at a toluene loading rate between 0.052 and 3.810 g m^{-3} and EBRTs of 1.2–2 min, obtaining a maximum EC of 93 g m⁻³ h⁻¹ at an inlet loading rate of 114 g m⁻³ h⁻¹ Despite the significantly higher ECs reported in these studies, toluene REs remained comparable, eventually exceeded 90 %. Regarding α -pinene, inlet loading rates were 0.17, 0.24, 0.30 and 0.46 g m⁻³ h⁻¹ at



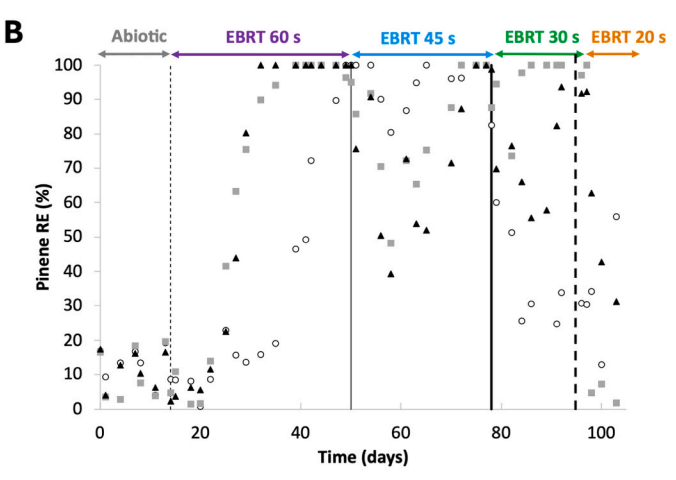


Fig. 7. Time course of the removal efficiencies of (A) toluene and (B) α -pinene in BTF-CP, (\blacksquare) BF-PSS and (\triangle) BTF-PSS-Fe under decreasing EBRTs. Vertical lines indicate changes in EBRT. Horizontal arrow lines at the upper part of the figure represent the empty bed residence time of the gas during this operational stage.

Table 5

Toluene and α -pinene steady state elimination capacities (EC; g m⁻³ h⁻¹) in the biofilters packed UgnCleanPellets®, compost and Fe-doped compost. Different superscripts indicate significant differences (p < 0.05).

Toluene EC (g $\mathrm{m}^{-3}~\mathrm{h}^{-1}$)						
EBRT (s)	BF-CP	BF-PSS	BF-PSS-Fe			
60	0.21 \pm 0.01 a	0.21 \pm 0.01 $^{\mathrm{a}}$	$0.22\pm0.01~^{a}$			
45	$0.26\pm0.01~^{a}$	$0.26\pm0.01~^{a}$	$0.27\pm0.00~^{a}$			
30	$0.38\pm0.01~^{a}$	$0.40\pm0.00~^a$	$0.40\pm0.00~^{a}$			
20	$0.53\pm0.00~^{a}$	$0.40\pm0.00^{\ \mathrm{b}}$	$0.41\pm0.03^{\text{ c}}$			

α-pinene EC (g $m^{-3} h^{-1}$)						
EBRT (s)	BF-CP	BF-PSS	BF-PSS-Fe			
60	0.17 \pm 0.01 a	$0.18\pm0.00~^{a}$	$0.18\pm0.01~^{a}$			
45	0.25 \pm 0.01 $^{\rm a}$	$0.24\pm0.02~^{a}$	$0.24\pm0.01~^a$			
30	$0.10\pm0.03~^{a}$	0.31 \pm 0.01 $^{\mathrm{b}}$	$0.27\pm0.02^{\ \mathrm{b}}$			
20	$0.19\pm0.02~^a$	$0.08\pm0.02^{\ b}$	$0.27\pm0.05~^{c}$			

EBRTs of 60, 45, 30 and 20 s, respectively. The maximum α-pinene EC was reached at different EBRTs depending on the packing material: 0.25 \pm 0.01 g m $^{-3}$ h $^{-1}$ in BF-CP at 45 s EBRT, 0.31 \pm 0.01 g m $^{-3}$ h $^{-1}$ in BF-PSS at 30 s EBRT, and 0.27 \pm 0.02 and 0.27 \pm 0.05 g m $^{-3}$ h $^{-1}$ in BF-PSS-Fe at EBRTs of 30 and 20 s, respectively. Similarly to toluene, the inlet loading rates of α-pinene in our study were lower than those reported in literature. Cabeza et al. (2013) assessed the performance of a 9.0 L BF packed with municipal solid waste compost both alone and mixed with pruning residues for the treatment of an α-pinene concentration of 11.6 ppm_v at an EBRT of 66 s. The maximum α-pinene ECs ranged between 79 and 113 g m $^{-3}$ h $^{-1}$, reaching REs > 90 %.

Overall, the results obtained for VOC biodegradation in BF-PSS-Fe were remarkably promising. The EBRTs typically reported in the literature for an effective VOCs removal in BFs are generally greater than those tested in this study, ranging from 120 to 60 s.

3.6. Influence of the EBRT on pressure drop across the BF packed bed

The pressure drop across the packed beds remained below 51.3 mm

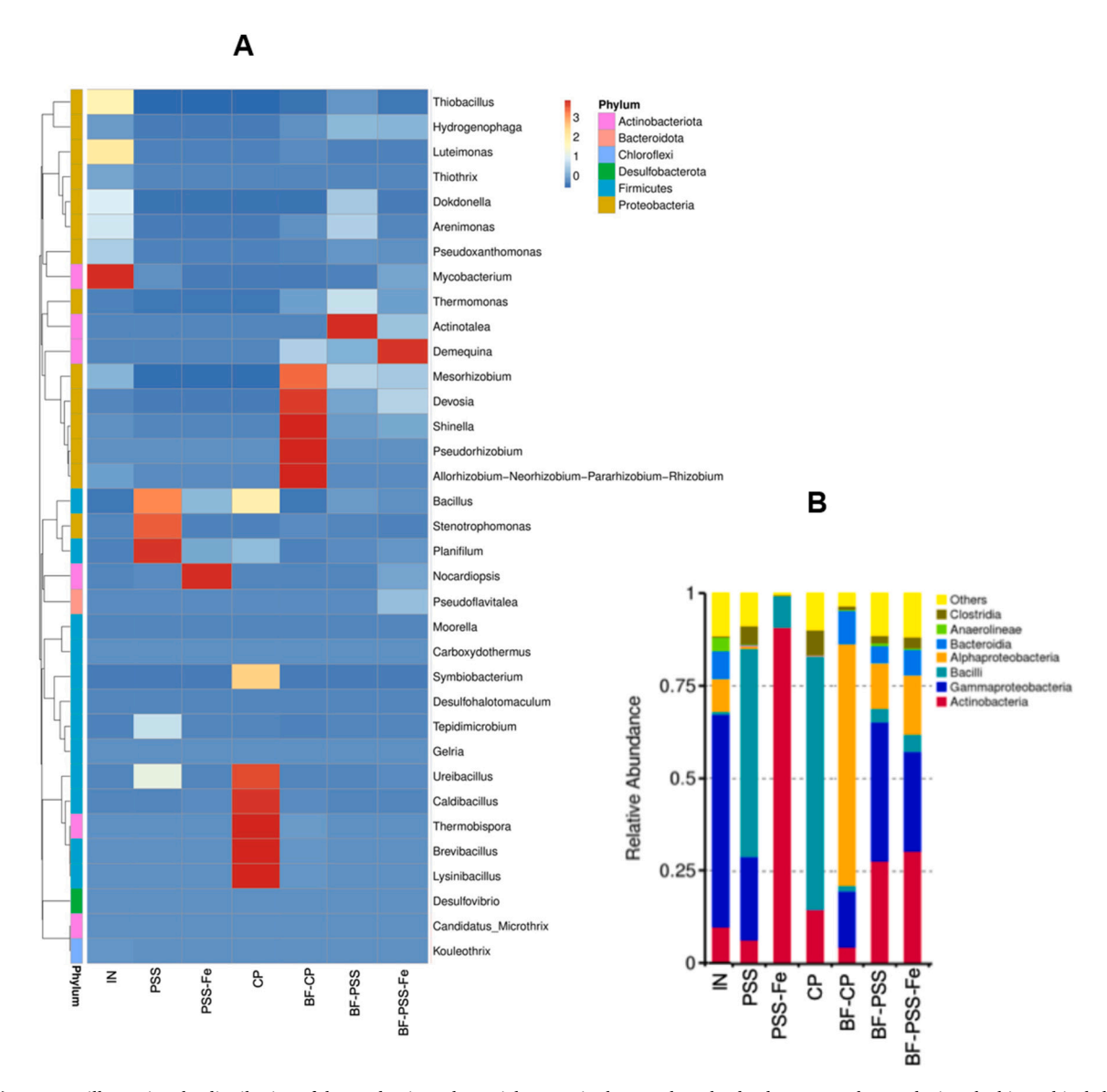


Fig. 8. (A) Heatmap illustrating the distribution of the predominant bacterial genera in the samples. The dendrogram at the top depicts the hierarchical clustering of the samples. Data are presented as relative abundance (%). (B) Bar plot of the main bacterial classes identified in each sample. IN refers to the inoculum, CP to the commercial pellet, PSS to the pelletised sewage sludge compost, PSS-Fe to the pelletised sewage sludge compost with high content of Fe salts. Similarly, BF-CP, BF-PSS and BF-PSS-Fe refer to samples drawn from the three BFs at the end of the experiment.

 $\mathrm{H_{2}O}\ \mathrm{m^{-1}}$ in the BF-CP and below 64.10 mm $\mathrm{H_{2}O}\ \mathrm{m^{-1}}$ in the BF-PSS and BF-PSS-Fe at EBRTs of 60, 45 and 30 s. Biofiltration for odour treatment typically operates at EBRTs ranging from 45 to 90 s, increasing to 120 s for the removal of VOCs, depending on the concentration and complexity of the compounds being treated. Within this typical EBRT operating range, the pressure drop in the BFs here tested was always lower than the 100 mm H_2O m⁻¹ value considered as the upper threshold for a cost-effective gas biofiltration (Delhoménie and Heitz, 2005). However, the step increase in the air flow rate led to higher pressure drops in the three BFs, with operational flooding problems appearing when operating the BFs at 20 s of EBRT. The high flow rate entailed pressure increases up to 244-, 974- and 436-mm H₂O m⁻¹ in BF-CP, BF-PSS and BF-PSS-Fe, respectively. At this point, structural differences were observed between CP and PSS/PSS-Fe as packing material. Previous literature studies have shown that the structural stability of packed beds can gradually deteriorate over time, and that pressure drop tends to increase approximately linearly with rising gas flowrates (Morgan-Sagastume et al., 2003).

3.7. Microbial community analysis

Sequence analysis was performed to compare the relative abundances of bacteria at the class and genus level. The 35 most prevalent bacterial species categorized by genus are shown in a heat map (Fig. 8-A).

The bacterial community analysis of CP, PSS and PSS-Fe pellets at the beginning of the experiment (before inoculation) showed differences in terms of abundance of the bacterial class (Fig. 8-B). The prevalent class in CP were Bacilli (68.3 %) and Actinobacteria (14.7 %), in PSS were Bacilli (56.1 %), Gammaproteobacteria (22.5 %) and Actinobacteria (6.5 %) and in PSS-Fe were Actinobacteria (90.8 %) and Bacilli (8.5 %). In terms of bacterial genus, the most representative genus belonged to Bacillus (14.7 %) in CP samples, while bacteria from the genus Thermobispora (9.3 %), Caldibacillus (7.8 %) and Brevibacillus (7.7 %) were also found. On the other hand, the main genus found in PSS were Bacillus (22.8 %) and Streptophomonas (19.6 %). Bacteria from the genus Planifilum (12.9 %), Tepidimicrobium (3.8 %), Delftia (2.4 %) and Geobacillus (2.3 %) were also identified. Interestingly, the presence of iron salts in the pelletised sewage sludge compost led to a substantial change in the bacterial community. Unlike in the other two samples, the most dominant bacteria identified belonged to the genus Nocardiopsis (84.9 %). Members of this genus are ecologically versatile, most of them being halotolerant or halophilic with prevalence in soils and marine environments (Bennur et al., 2016). Nocardiopsis species produce an array of bioactive compounds such as antimicrobial agents, toxins and immunomodulators (Bennur et al., 2015). Bacteria of the genus Bacillus were also identified in PSS-Fe (4.2 %), along with microorganisms from the genus Planifilum (1.2 %), Thermobifida (1.2 %), Stackebrandtia (1.6 %) and Sporosarcina (1.4 %).

The dominant class in the inoculum of the BFs was *Gammaproteobacteria* (57.5 %) (Fig. 8-B). Since the inoculum was previously acclimated to the biodegradation of odorous compounds, bacteria associated to SOB and VOC biodegradation were identified. *Thiobacillus* (28.9 %), belonging to the group of SOB, plays a major role in the sulphur cycle (Gerrity et al., 2016). Other detected bacteria known for VOC degradation included *Mycobacterium* (6.0 %), *Pseudoxanthomonas* (4.4 %), *Luteimonas* (3.3 %), *Dokdonella* (2.8 %) and *Rhodococcus* (1.2 %) (González-Martín et al., 2024) (Yamaguchi et al., 2018) (Kastner et al., 1999). Additionally, *Nitrosomas* (2.6 %), an ammonia-oxidizing bacteria, was detected in the inoculum.

After 93 days of experimentation, the microbial community of the three BFs changed significantly. Interestingly, BF-PSS and BF-PSS-Fe showed similar microbial structure in terms of class of bacteria. The most abundant classes belonged to *Gammaproteobacteria* (37.5 % and 26.8 %), *Actinobacteria* (27.7 % and 30.4 %) and *Alphaproteobacteria* (12.2 and 15.9 %) in BF-PSS and BF-PSS-Fe, respectively. In BF-CP, the

dominant classes were *Alphaproteobacteria* (65.1 %) and *Gammaproteobacteria* (15.1 %) (Fig. 8-B).

In terms of bacterial genus, the most abundant microorganisms in BF-CP belonged to the genus *Devosia* (24.4 %). *Shinella* (5.7 %), *Pseudorhizobium* (5.4 %), *Thermomonas* (4.1 %) and *Thiobacillus* (1.3 %) were also present in the BF-CP. Conversely, the predominant bacteria in BF-PSS corresponded to the genus *Thermomonas* (12.2 %), with bacteria from the genus *Thiobacillus* (5.2 %), *Actinotalea* (5.5 %), *Cellulosimicrobium* (3.9 %), *Bacillus* (2.2 %) and *Devosia* (2.1 %) being also identified. Finally, the microbial community present in the BF-PSS-Fe at the end of the experiment belonged to the genus *Nocardiopsis* (6.3 %), *Devosia* (5.7 %), *Demequina* (4.9 %), *Leptonema* (4.2 %), *Thermomonas* (3.8 %) and *Thiobacillus* (1.8 %).

Three bacterial genera were consistently detected across all biofilters, although with varying relative abundances. Among them, Thiobacillus, a sulphur-oxidizing bacterium (SOB) responsible for the conversion of HS⁻ to SO₄²⁻ (Kumar et al., 2020), was present in all systems. Likewise, both ammonia-oxidizing bacteria (AOB) and nitriteoxidizing bacteria (NOB) were identified. Nitrospira, capable of oxidizing both ammonia and nitrite (Vijayan et al., 2021), was found at relative abundances of 0.5 %, 0.2 %, and 0.4 % in BF-CP, BF-PSS, and BF-PSS-Fe, respectively. Nitrosomonas (AOB) was also detected, with relative abundances of 0.2 %, 0.7 %, and 0.1 % in the same systems. Devosia, an aerobic bacterium associated with nitrogen fixation and the degradation of organic sulphur, phosphorus, and aromatic compounds (Talwar et al., 2020), was also present in all biofilters. In terms of VOCdegrading bacteria, members of the genera Pseudoxanthomonas (0.1 %, 0.9 %, and 0.8 % in BF-CP, BF-PSS, and BF-PSS-Fe, respectively), Dokdonella (0.03 %, 1.8 %, and 0.2 %), and Rhodococcus (0.1 %, 0.1 %, and 0.8%) were identified. These genera are widely recognised for their role in VOC biodegradation (González-Martín et al., 2024; Yamaguchi et al., 2018; Wu et al., 2018).

Since all three biofilters were operated under identical conditions, including pollutant concentrations, loading rates, MSM irrigation, and temperature, the observed differences in microbial composition are likely due to the distinct chemical and physical properties of the packing materials, as well as the native microbiota associated with each pellet type. These material-specific properties may also influence microbial colonisation and biofilm formation. Nevertheless, despite variations in microbial abundance across the systems, several genera, such as *Thermomonas, Thiobacillus, Pseudoxanthomonas, Dokdonella*, and *Devosia*, were shared by all biofilters, indicating a core community involved in the degradation of the target pollutants.

4. Conclusions

This research demonstrates a practical application of circular economy principles within the integrated water cycle by valorising WWTP sludge by-products (specifically sewage sludge compost and Fe-enriched sewage sludge compost) as effective packing materials in biofiltration systems for odour and VOC abatement. All tested bed materials achieved a complete removal of H2S and NH3. However, the Fe-doped pelletised sewage sludge compost clearly outperformed the commercial irondoped clay pellets in the removal of VOCs, particularly at low EBRT (30 s), with REs exceeding 99 % for toluene and 92 % for α -pinene. These results are significant as they indicate that BFs packed with this wastederived material not only match but surpass the performance of conventional commercial media, while operating efficiently at shorter residence times than typically reported for VOC abatement, thereby reducing both the operational footprint and treatment costs. Moreover, the Fe-doped pelletised sewage sludge compost promoted the growth of bacterial genera known for their roles in the biodegradation of reduced sulphurous and nitrogenous compounds, as well as VOCs, such as Nocardiopsis, Devosia, Thermomonas, Thiobacillus, Nistrospira and Rhodococcus, further supporting its effectiveness. Overall, this work contributes to both environmental biotechnology and circular waste

management by offering a low-cost, sustainable and technically superior solution for gaseous emission control in WWTPs and other odour-emitting facilities.

CRediT authorship contribution statement

S. Sáez-Orviz: Writing – original draft, Methodology, Investigation, Formal analysis, Data curation. R. Lebrero: Writing – review & editing, Supervision, Investigation, Funding acquisition, Conceptualization. L. Terrén: Writing – review & editing, Funding acquisition, Conceptualization. S. Doñate: Writing – review & editing, Funding acquisition, Conceptualization. M.D. Esclapez: Writing – review & editing, Funding acquisition, Conceptualization. L. Saúco: Writing – review & editing, Funding acquisition, Conceptualization. R. Muñoz: Writing – review & editing, Supervision, Investigation, Funding acquisition, Conceptualization.

Declaration of competing interest

The authors declare that there are no conflicts of interests in the submission and publication of this manuscript.

Acknowledgements

This research was partially funded by The Centre for the Development of Industrial Technology (CDTI) and supported by the Regional Government of Castilla y León (UIC 379).

Appendix A. Supplementary data

Supplementary data to this article can be found online at https://doi.org/10.1016/j.scitotenv.2025.179927.

Data availability

No data was used for the research described in the article.

References

- Barbusinski, K., Kalemba, K., Kasperczyk, D., Urbaniec, K., Kozik, V., 2017. Biological methods for odor treatment – a review. J. Clean. Prod. 152, 223–241. https://doi. org/10.1016/j.jclepro.2017.03.093.
- Bennur, T., Kumar, A.R., Zinjarde, S., Javdekar, V., 2015. Nocardiopsis species: incidence, ecological roles and adaptations. Microbiol. Res. 174, 33–47. https://doi. org/10.1016/j.micres.2015.03.010.
- Bennur, T., Ravi Kumar, A., Zinjarde, S.S., Javdekar, V., 2016. Nocardiopsis species: a potential source of bioactive compounds. J. Appl. Microbiol. 120, 1–16. https://doi. org/10.1111/jam.12950.
- Bharathi, P.A., L., 2018. Sulfur cycle. Encycl. Ecol. Vol. 1-4. Second Ed. 4, 192–199. https://doi.org/10.1016/B978-0-444-63768-0.00761-7.
- Bokowa, A., Diaz, C., Koziel, J.A., McGinley, M., Barclay, J., Schauberger, G., Guillot, J. M., Sneath, R., 2021. Short introduction to the summary and evaluation of the odour regulations worldwide. Chem. Eng. Trans. https://doi.org/10.3303/CET2185021.
- Cabeza, I.O., López, R., Giraldez, I., Stuetz, R.M., Díaz, M.J., 2013. Biofiltration of α-pinene vapours using municipal solid waste (MSW) pruning residues (P) composts as packing materials. Chem. Eng. J. 233, 149–158. https://doi.org/10.1016/j.cej.2013.08.032.
- Cantera, S., López, M., Muñoz, R., Lebrero, R., 2022. Chemosphere comparative evaluation of bacterial and fungal removal of indoor and industrial polluted air using suspended and packed bed bioreactors. Chemosphere 308, 0–10. https://doi.org/10.1016/j.chemosphere.2022.136412.
- Chaudhary, D.K., Park, J.H., Kim, P.G., Ok, Y.S., Hong, Y., 2023. Enrichment cultivation of VOC-degrading bacteria using diffusion bioreactor and development of bacterialimmobilized biochar for VOC bioremediation. Environ. Pollut. 320, 121089. https:// doi.org/10.1016/j.envpol.2023.121089.
- Chen, X., Sun, P., Zhuang, Z., Ahmed, I., Zhang, L., Zhang, B., 2024. Control of odorants in swine manure and food waste co-composting via zero-valent iron /H2O2 system. Waste Manag. 174, 390–399. https://doi.org/10.1016/j.wasman.2023.12.018.
- Cheng, Z., Lu, L., Kennes, C., Yu, J., Chen, J., 2016. Treatment of gaseous toluene in three biofilters inoculated with fungi/bacteria: microbial analysis, performance and starvation response. J. Hazard. Mater. 303, 83–93. https://doi.org/10.1016/j. jhazmat.2015.10.017.

- Czarnota, J., Masloń, A., Pajura, R., 2023. Wastewater treatment plants as a source of malodorous substances hazardous to health, including a case study from Poland. Int. J. Environ. Res. Public Health 20, 5379. https://doi.org/10.3390/ijerph20075379.
- Delhoménie, M.C., Heitz, M., 2005. Biofiltration of air: a review. Crit. Rev. Biotechnol. 25, 53–72. https://doi.org/10.1080/07388550590935814.
- Dinçer, F., Dinçer, F.K., Sarı, D., Ceylan, O., Ercan, Ö., 2020. Dispersion modelling and air quality measurements to evaluate the odor impact of a wastewater treatment plant in Izmir. Atmos. Pollut. Res. https://doi.org/10.1016/j.apr.2020.05.018.
- Edgar, R.C., 2013. UPARSE: highly accurate OTU sequences from microbial amplicon reads. Nat. Methods 10, 996–998. https://doi.org/10.1038/nmeth.2604.
- Gao, L., Keener, T.C., Zhuang, L., Siddiqui, K.F.A., 2001. A technical and economic comparison of biofiltration and wet chemical oxidation (scrubbing) for odour control at wastewater treatment plants. Environ. Eng. Policy. 2, 203–212.
- Gerrity, S., Kennelly, C., Clifford, E., Collins, G., 2016. Hydrogen sulfide oxidation in novel horizontal-flow biofilm reactors dominated by an Acidithiobacillus and a Thiobacillus species. Environ. Technol. (United Kingdom) 37, 2252–2264. https:// doi.org/10.1080/09593330.2016.1147609.
- Godoi, A.F.L., Grasel, A.M., Polezer, G., Brown, A., Potgieter-Vermaak, S., Camargo Scremim, D., Yamamoto, C.I., Moreton Godoi, R.H., 2018. Human exposure to hydrogen sulphide concentrations near wastewater treatment plants. Sci. Total Environ. https://doi.org/10.1016/j.scitotenv.2017.07.209.
- González-Martín, J., Cantera, S., Muñoz, R., Lebrero, R., 2024. Indoor air VOCs biofiltration by bioactive coating packed bed bioreactors. J. Environ. Manag. 349. https://doi.org/10.1016/j.jenvman.2023.119362.
- Gupta, R.K., Poddar, B.J., Nakhate, S.P., Chavan, A.R., Singh, A.K., Purohit, H.J., 2021. Role of heterotrophic nitrifiers and aerobic denitrifiers in simultaneous nitrification and denitrification process: a nonconventional nitrogen removal pathway in wastewater treatment. https://doi.org/10.1111/lam.13553.
- Holmes, D.E., Dang, Y., Smith, J.A., 2018. Nitrogen cycling during wastewater treatment. In: Advances in Applied Microbiology, 1st ed. Elsevier Inc. https://doi.org/10.1016/bs.aambs.2018.10.003
- Kampa, M., Castanas, E., 2008. Human health effects of air pollution 151, 362–367. https://doi.org/10.1016/j.envpol.2007.06.012.
- Kastner, J.R., Thompson, D.N., Cherry, R.S., 1999. Water-soluble polymer for increasing the biodegradation of sparingly soluble vapors. Enzym. Microb. Technol. 24, 104–110. https://doi.org/10.1016/S0141-0229(98)00108-2.
- Kleinheinz, G.T., Bagley, S.T., St. John, W.P., Rughani, J.R., McGinnis, G.D., 1999. Characterization of alpha-pinene-degrading microorganisms and application to a bench-scale biofiltration system for VOC degradation. Arch. Environ. Contam. Toxicol. 37, 151–157. https://doi.org/10.1007/s002449900500.
- Kumar, M., Zeyad, M.T., Choudhary, P., Paul, S., Chakdar, H., Rajawat, M.V.S., 2020. Thiobacillus. Benef. Microbes Agro-Ecology Bact. Fungi 545–557. https://doi.org/10.1016/B978-0-12-823414-3.00026-5.
- Lebrero, R., Gondim, A.C., Pérez, R., García-Encina, P.A., Muñoz, R., 2014. Comparative assessment of a biofilter, a biotrickling filter and a hollow fiber membrane bioreactor for odor treatment in wastewater treatment plants. Water Res. 49, 339–350. https:// doi.org/10.1016/j.watres.2013.09.055.
- Lebrero, R., Rangel, M.G.L., Muñoz, R., 2013. Characterization and biofiltration of a real odorous emission from wastewater treatment plant sludge. J. Environ. Manag. 116, 50–57. https://doi.org/10.1016/j.jenvman.2012.11.038.
- Lebrero, R., Rodríguez, E., Collantes, M., De Juan, C., Norden, G., Rosenbom, K., Muñoz, R., 2021. Comparative performance evaluation of commercial packing materials for malodorants abatement in biofiltration. Appl. Sci. 11. https://doi.org/ 10.3390/app11072966.
- Lim, E., Mbowe, O., Lee, A.S.W., Davis, J., Lim, E., Mbowe, O., Lee, A.S.W., Effect, J.D., Lim, E., Mbowe, O., Lee, A.S.W., Davis, J., 2016. Effect of environmental exposure to hydrogen sulfide on central nervous system and respiratory function: a systematic review of human studies 3525. https://doi.org/10.1080/10773525.2016.1145881.
- Luckert, A., Aguado, D., García-Bartual, R., Lafita, C., Montoya, T., Frank, N., 2023. Odour mapping and air quality analysis of a wastewater treatment plant at a seaside tourist area. Environ. Monit. Assess. 195 (8), 1013. https://doi.org/10.1007/ s10661-023-11598-8.
- Magoč, T., Salzberg, S.L., 2011. FLASH: fast length adjustment of short reads to improve genome assemblies. Bioinformatics 27, 2957–2963. https://doi.org/10.1093/bioinformatics/htr507
- Márquez, P., Herruzo-Ruiz, A.M., Siles, J.A., Alhama, J., Michán, C., Martín, M.A., 2021. Influence of packing material on the biofiltration of butyric acid: a comparative study from a physico-chemical, olfactometric and microbiological perspective. J. Environ. Manag. 294. https://doi.org/10.1016/j.jenvman.2021.113044.
- Morgan-Sagastume, J.M., Noyola, A., Revah, S., Ergas, S.J., 2003. Changes in physical properties of a compost biofilter treating hydrogen sulfide. J. Air Waste Manage. Assoc. 53, 1011–1021. https://doi.org/10.1080/10473289.2003.10466249.
- Pachaiappan, R., Cornejo-Ponce, L., Rajendran, R., Manavalan, K., Femilaa Rajan, V., Awad, F., 2022. A review on biofiltration techniques: recent advancements in the removal of volatile organic compounds and heavy metals in the treatment of polluted water. Bioengineered 13, 8432–8477. https://doi.org/10.1080/ 21655979.2022.2050538.
- Pan, C., Yang, H., Gao, W., Wei, Z., Song, C., Mi, J., 2024. Optimization of organic solid waste composting process through iron-related additives: a systematic review. J. Environ. Manag. 351, 119952. https://doi.org/10.1016/j.jenvman.2023.119952.
- Park, B.-G., Shin, W.-S., Chung, J.-S., 2008. Simultaneous biofiltration of H 2 S, NH 3 and toluene using an inorganic/polymeric composite carrier. Environ. Eng. Res. 13, 19–27. https://doi.org/10.4491/eer.2008.13.1.019.
- Quast, C., Pruesse, E., Yilmaz, P., Gerken, J., Schweer, T., Yarza, P., Peplies, J., Glöckner, F.O., 2013. The SILVA ribosomal RNA gene database project: improved

- data processing and web-based tools. Nucleic Acids Res. 41, 590–596. https://doi.
- Rabbani, K.A., Charles, W., Kayaalp, A., Cord-Ruwisch, R., Ho, G., 2016. Pilot-scale biofilter for the simultaneous removal of hydrogen sulphide and ammonia at a wastewater treatment plant. Biochem. Eng. J. 107, 1–10. https://doi.org/10.1016/j. hei 2015 11 018
- Rajamanickam, R., Baskaran, D., 2017. Biodegradation of gaseous toluene with mixed microbial consortium in a biofilter: steady state and transient operation. Bioprocess Biosyst. Eng. 40, 1801–1812. https://doi.org/10.1007/s00449-017-1834-7.
- Ren, B., Zhao, Y., Lyczko, N., Nzihou, A., 2019. Current status and outlook of odor removal Technologies in Wastewater Treatment Plant. Waste Biomass Valoriz. 10, 1443–1458. https://doi.org/10.1007/s12649-018-0384-9.
- Rene, E.R., Sergienko, N., Goswami, T., López, M.E., Kumar, G., Saratale, G.D., Venkatachalam, P., Pakshirajan, K., Swaminathan, T., 2018. Effects of concentration and gas flow rate on the removal of gas-phase toluene and xylene mixture in a compost biofilter. Bioresour. Technol. 248, 28–35. https://doi.org/10.1016/j. biortech.2017.08.029.
- Sáez-Orviz, S., Lebrero, R., Terrén, L., Doñate, S., Esclapez, M.D., Saúco, L., Muñoz, R., 2024. Evaluation of the performance of new plastic packing materials from plastic waste in biotrickling filters for odour removal. Process. Saf. Environ. Prot. 191, 2361–2372. https://doi.org/10.1016/j.psep.2024.10.009.
- Sheoran, K., Siwal, S.S., Kapoor, D., Singh, N., Saini, A.K., Alsanie, W.F., Thakur, V.K., 2022. Air pollutants removal using biofiltration technique: a challenge at the Frontiers of sustainable environment. ACS Eng. Au 2, 378–396. https://doi.org/10.1021/acsengineeringau.2c00020.
- Talwar, C., Nagar, S., Kumar, R., Scaria, J., Lal, R., Negi, R.K., 2020. Defining the environmental adaptations of genus Devosia: insights into its expansive short peptide transport system and positively selected genes. Sci. Rep. 10, 1–18. https:// doi.org/10.1038/s41598-020-58163-8.

- U.S. Department of Labor, Occupational Safety and Health Administration. (n.d.).
 Hydrogen sulfide -Hazards. Occupational Safety and Health Administration. https://www.osha.gov/hydrogen-sulfide/hazards.
- Vela-Aparicio, D.G., Forero, D.F., Fernandez, A., Hernandez, M.A., Brandão, P.F.B., Cabeza, I.O., 2021. Operational parameters analysis for the removal of H2S and NH3under transient conditions by a biofiltration system of compost beds. Chem. Eng. Trans. 85, 163–168. https://doi.org/10.3303/CET2185028.
- Vijayan, A., Vattiringal Jayadradhan, R.K., Pillai, D., Prasannan Geetha, P., Joseph, V., Isaac Sarojini, B.S., 2021. Nitrospira as versatile nitrifiers: taxonomy, ecophysiology, genome characteristics, growth, and metabolic diversity. J. Basic Microbiol. 61, 88–109. https://doi.org/10.1002/jobm.202000485.
- Vikrant, K., Kailasa, S.K., Tsang, D.C.W., Lee, S.S., Kumar, P., Giri, B.S., Singh, R.S., Kim, K.H., 2018. Biofiltration of hydrogen sulfide: trends and challenges. J. Clean. Prod. 187, 131–147. https://doi.org/10.1016/j.jclepro.2018.03.188.
- Wu, H., Guo, C., Yin, Z., Quan, Y., Yin, C., 2018. Performance and bacterial diversity of biotrickling filters filled with conductive packing material for the treatment of toluene. Bioresour. Technol. 257, 201–209. https://doi.org/10.1016/j. biortech.2018.02.108.
- Yamaguchi, Tsuyoshi, Nakamura, S., Hatamoto, M., Tamura, E., Tanikawa, D., Kawakami, S., Nakamura, A., Kato, K., Nagano, A., Yamaguchi, Takashi, 2018. A novel approach for toluene gas treatment using a downflow hanging sponge reactor. Appl. Microbiol. Biotechnol. 102, 5625–5634. https://doi.org/10.1007/s00253-018-8933-5.
- Zhao, X., 2018. IOP Conf, 153. Earth Environ. Sci, Ser, p. 022014.
- Zhu, R., Li, S., Bao, X., Dumont, É., 2017. Comparison of biological H2S removal characteristics between a composite packing material with and without functional microorganisms. Sci. Rep. 7, 1–8. https://doi.org/10.1038/srep42241.